A Wavelet-Based Algorithm to Estimate Ocean Wave Group Parameters From Radar Images

Andreas Niedermeier, José Carlos Nieto Borge, Susanne Lehner, *Member, IEEE*, and Johannes Schultz-Stellenfleth

***Abstract*—In recent years, new remote sensing techniques have been developed to measure two-dimensional (2-D) sea surface elevation fields. The availability of these data has led to the necessity to extend the classical analysis methods for one-dimensional (1-D) buoy time series to two dimensions. This paper is concerned with the derivation of group parameters from 2-D sea surface elevation fields using a wavelet-based technique. Wave grouping is known to be an important factor in ship and offshore safety, as it plays a role in dangerous resonance phenomenons and the generation of extreme waves. Synthetic aperture radar (SAR) data are used for the analysis. The wavelet technique is introduced using synthetic ocean surfaces and simulated SAR data. It is shown that the group structure of the ocean wave field can be recovered from the SAR image if the nonlinear imaging effects are moderate. The method is applied to a global dataset of European Remote Sensing satellite (ERS-2) wave mode data. Different group parameters including the area covered by the largest group and the number of groups in a given area are calculated for over 33 000 SAR images. Global maps of the parameters are presented. For comparison, classical 1-D grouping parameters are calculated from colocated wave model data showing good overall agreement with the wavelet-derived parameters. ERS-2 image mode data are used to study wave fields in coastal areas. Waves approaching the island of Sylt in the North Sea are investigated, showing the potential of the wavelet technique to analyze the spatial wave dynamics associated with the bottom topography. Observations concerning changes of wavelength and group parameters are compared to linear wave theory.**

***Index Terms*—Edge detection, group parameters, imagettes, ocean waves, synthetic aperture radar (SAR), wavelets.**

I. Introduction

In RECENT years, a number of new remote sensing techniques based on both optical and radar data have been developed to estimate two-dimensional (2-D) sea surface elevation fields [1]–[4]. Compared to the traditional buoy time series, the data provide a wealth of new information, which is of practical as well as of theoretical interest.

The practical relevance lies in the fact that state-of-the-art techniques used in the design of ships and offshore structures require detailed 2-D information on the sea surface to estimate the respective response of the marine structure [5]. The scientific interest, on the other hand, is motivated by the fact that there are strong indications that important dynamical processes, like, for example, the formation of extreme waves are strongly conditioned by 2-D properties of the wave field [6], [7].

In this paper, the focus is on ocean wave grouping, which is one important characteristic 2-D property of the sea surface. Ocean waves tend to form wave groups [8]–[10], which are characterized by sequences of high waves with nearly equal wavelengths. Wave groups often cause serious damage to ships, as well as to offshore structures. That occurs when the period of each individual wave in the group is close to the resonance period of the marine structure [11]. Many studies of wave groupiness have been carried out for wave elevation time series recorded by *in situ* sensors, such buoys [12], [13], as well as results obtained from laboratory observations [14]. These studies analyze primarily the occurrence of the wave groupiness phenomenon in one dimension (e.g., the temporal domain). This one-dimensional (1-D) description of wave groupiness can be complemented using the new remote sensing systems mentioned above, which are able to describe the sea surface variability in two dimensions (e.g., the spatial domain).

To study wave grouping, high-resolution images acquired by spaceborne synthetic aperture radar (SAR) are used in this study. It has been demonstrated that SAR is an efficient instrument to analyze wave fields in the open ocean [15], [16]. Although SAR has some limitations with regard to the imaging of waves traveling in the satellite flight direction (azimuth), it is still the only instrument capable of providing directional ocean wave information on a global scale. So far, however, SAR data have been mainly used to estimate the 2-D wave spectrum [17], i.e., the spatial information provided by SAR was not fully exploited.

The present work deals with the analysis of wave groups in the spatial domain from SAR images of wave fields. The method developed to determine wave groups from SAR images is based on a SAR edge detection algorithm [18]. This method uses a wavelet edge detection, which permits to separate regions of contiguous higher waves from other regions where the individual waves are lower than a given threshold. Hence, this technique determines group run areas, as well as their spatial variability, within SAR images, using only the image information.

This wavelet-based technique is applied to a dataset composed of more than 33 000 SAR measurements globally distributed. Each SAR measurement was taken by the European Remote Sensing satellite (ERS-2) in its so-called *wave mode*. Hence, taking into account the amount of SAR measurements over the ocean (i.e., more than ten years of continuous observation), the use of spaceborne SAR images allows to characterize wave group features for different seasons on a global scale.

Manuscript received April 30, 2004; revised August 3, 2004. This work was supported by the European Union in the framework of the MAXWAVE project.

A. Niedermeier, J. C. N. Borge, and J. Schulz-Stellenfleth are with the Remote Sensing Technology Institute, German Aerospace Center (DLR), D-82234 Oberpfaffenhofen, Germany (e-mail: Andreas.Niedermeier@dlr.de; Jose.C.Nieto@dlr.de; Johannes.Schulz-Stellenfleth@dlr.de).

S. Lehner is with the Rosenstiel School of Marine and Atmospheric Science, University of Miami, Miami, FL 33149-1098 USA (e-mail: slehner@rsmas.miami.edu).

Digital Object Identifier 10.1109/TGRS.2004.836873

TABLE I
TIME PERIODS AND APPROXIMATE NUMBER OF IMAGETTES

time period	number
Aug. 21–Sep. 8,1996	25600
October 4–8, 1996	6200
June 1–2, 1997	1600

The paper is structured as follows. Section II describes the SAR datasets used. In Section III, basics of the SAR imaging mechanism of ocean waves are described, while Section IV gives an introduction to wave group analysis in one dimension. Section V explains the new wavelet grouping detection method. Results from some exemplary images are presented. Section VI gives statistical analysis of the new 2-D wave group definition in comparison to historic wave group parameters on a global scale. Analysis of wave grouping in coastal areas is presented in Section VII based on ERS-2 image mode data. Finally, Section VIII contains the conclusions.

II. DATASET

The dataset used in this work consists of approximately 33 000 ERS-2 SAR imagettes acquired in 1996–1997, and the acquisition periods and respective number of imagettes are given in Table I. The SAR raw data of approximately three weeks in total were processed to obtain the complex SAR intensity images using the German Aerospace Center (DLR) BSAR processor [19]. The imagettes are about 5×10 km^2 in size, where the spatial resolution is 10 m in azimuth and 20 m in range. They are distributed globally in the open ocean along the ERS-2 orbits, with a separation between consecutive acquisitions of 200 km. Some examples of these imagettes are presented in Fig. 1.

Fig. 2 gives a rough idea of its coverage and distribution of the data. The number of imagettes within each $3^\circ \times 3^\circ$ grid area is given for the three-week dataset.

For regional comparison, a dataset of Wave Model (WAM) spectra from the European Centre for Medium-Range Weather Forecasts (ECMWF) of the same time periods is used to derive classical wave grouping parameters.

III. SAR IMAGING OF OCEAN WAVES

Spaceborne SAR is still the only sensor capable of providing 2-D sea surface information on a global scale [16], [20]. A SAR uses the Doppler shifts of the returned signals to obtain a high resolution in the flight direction (azimuth) over stationary terrain. For a moving sea surface, this mechanism causes the wave patterns seen on SAR images to appear distorted with respect to the underlying ocean wave field. Apart from some details regarding the so-called real aperture radar (RAR) modulation mechanism, the SAR ocean wave imaging is well understood by now, and physical models describing the mapping process have been developed [21].

In particular, for azimuthal traveling waves, the SAR imaging process is often highly nonlinear, which can make it impossible to reverse the distortions caused by motions effects without having additional information available. To quantify the degree of nonlinearity the parameter C_{lin} was introduced in [22], which in case of a single harmonic wave system can be written as

$$C_{\mathrm{lin}} \approx \sqrt{\frac{2\pi g}{\lambda^3}} \frac{R}{v} \frac{H_s}{4} \sin\varphi \tag{1}$$

where λ, φ, and H_s are the peak wavelength, propagation direction relative to the look direction of the SAR antenna (range direction), and significant waveheight height. The range to velocity term is $R/v \approx 111$ s in case of the ERS-1/2, and $g = 9.81$ ms^{-2} is the gravitational acceleration. It was shown in [22] that a linear approximation of the SAR imaging mechanism is feasible for $C_{\mathrm{lin}} < 0.7$, which is the case for longer waves traveling close to range direction.

For waves traveling in range direction, the imaging process is dominated by the so-called tilt modulation mechanism [16]. Basically, this means that the SAR wave patterns are approximately 90° phase shifted toward the radar with respect to the underlying ocean waves. In this study, we will concentrate on these cases where the imaging distortions are moderate, enabling the extraction of information on the ocean wave field structure from the SAR image directly. It is well known that hydrodynamic effects play an additional role in the SAR imaging process. However, as the impact is relatively small compared to the tilt effect and also the corresponding phase shift is only known with poor accuracy, we neglect this effect in the present study.

For the special case of range traveling ocean waves, we consider a Gaussian wave group that satisfies the linear wave theory [23] and which can be written as

$$\eta(x,t) = \frac{A}{\sqrt{D}} e^{-((2\overline{\omega}B/gD)(x-(gt/2\overline{\omega})))^2} \cdot \cos\left(\frac{(\overline{\omega}^2 - 4B^4t^2)x - \overline{\omega}tg}{D^2 g} + \frac{1}{2}\tan^{-1}\frac{4B^2x}{g}\right) \tag{2}$$

where $D = \sqrt{1 + (16B^4x^2/g^2)}$, A is the maximum amplitude, B is the envelope decay constant, and $\overline{\omega}$ is the carrier frequency of the group. To illustrate the SAR imaging process, we use a sea surface composed of two range traveling wave groups $\eta(x - x_j, t_j)$ located at different positions (x_j, t_j) $(j = 1, 2)$. The curve at the top of Fig. 3 shows a cut through the ocean surface in range direction.

The respective normalized SAR intensity image of the two groups is shown in the center of Fig. 3. An incidence angle of 23° with sensor looking from the right was assumed. The exact analytical expressions for the tilt transfer function can be found in [16]. The gray curve in the center of Fig. 3 demonstrates the additional effect of speckle noise to be expected from a five-look averaged SAR image. The positions marked by the gray bars correspond to the group runs found by the algorithm presented in Section V.

The important thing to note here is that for the range traveling case, the group structure of the wave field, i.e., the size and the relative position of the groups, is well represented in the SAR image. This observation provides the justification for the image analysis presented in Sections IV–VII.

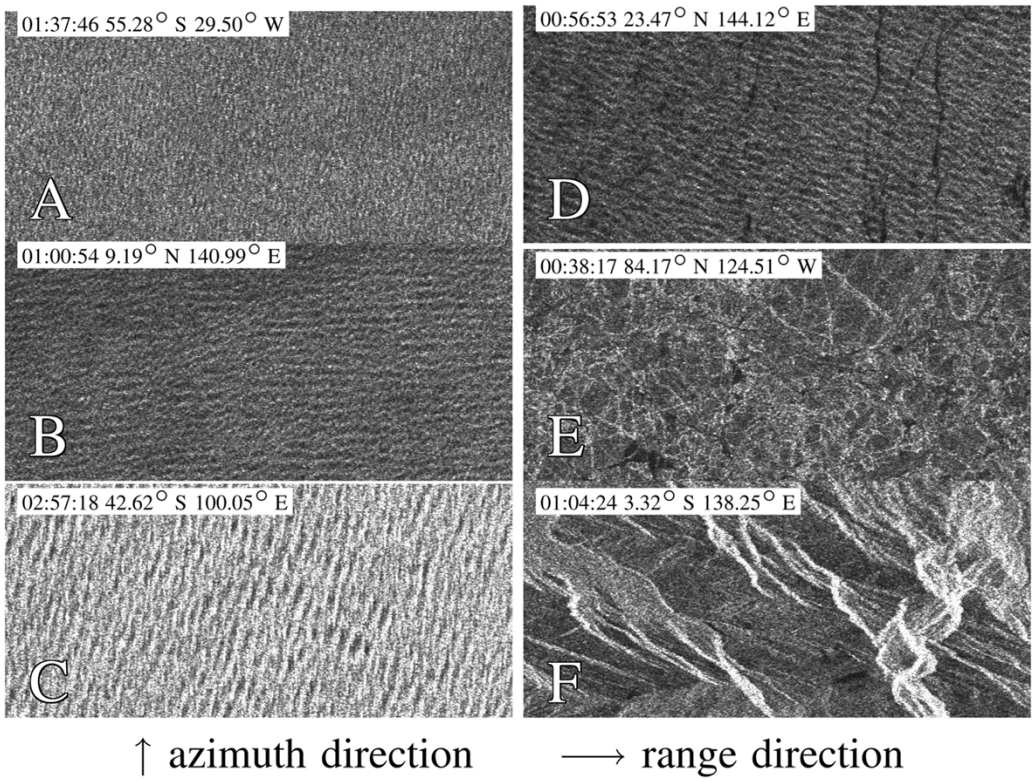

Fig. 1. Some exemplary ERS-2 imagettes showing waves propagating in range (a) and azimuth (b) direction, strong wave grouping (c), surface slicks (d), sea ice (e), and land (f). The images were taken on Oct. 6, 1996 with exact acquisition times and locations given in the figures.

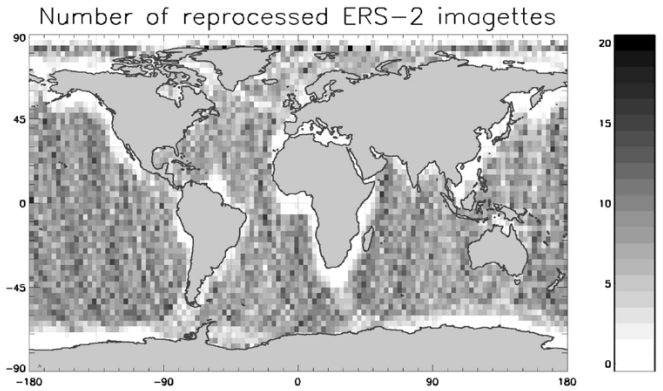

Fig. 2. Number of ERS-2 imagettes per $3^\circ \times 3^\circ$ grid area for the time period given in Table I.

IV. Wave Group Analysis in One Dimension

A group is defined as a sequence of waves with nearly equal periods [24], [25]. The analysis of wave groups has been traditionally carried out in one dimension based on wave elevation time series measured by buoys anchored at fixed positions of the ocean. Considering these wave elevation time series as a realization of a stochastic process, different methods to describe groupiness properties have been carried out [12], [13].

These methods fall into two main categories. The first approach considers the phenomenon as a threshold-crossing problem [26]–[30]. Here, the groups are characterized by the number of consecutive waves exceeding a given threshold H_0, which is typically chosen as the significant wave height

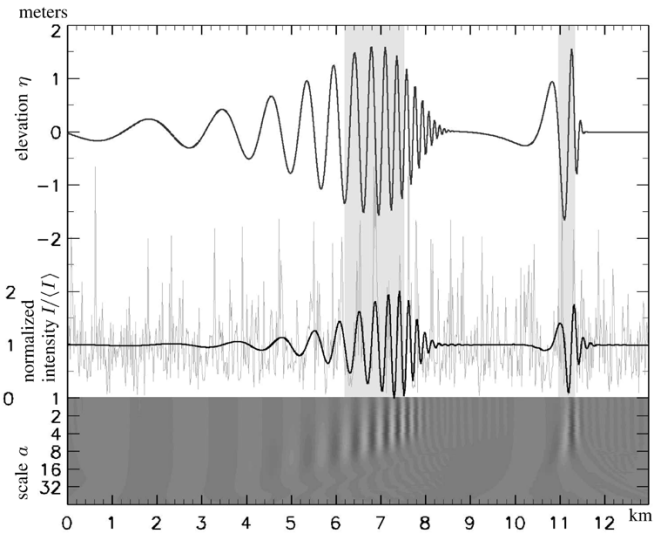

Fig. 3. Two Gaussian wave groups (top) propagating in range direction and the respective normalized SAR intensity image. The image at the bottom shows the wavelet transform of the simulated SAR image without speckle for wavelet scales $a \in [1, 64]$. Bright intensities correspond to positive values and vice versa.

H_s or the mean waveheight $\bar{H}$. In the scientific literature, the succession of waves satisfying this condition is known as a run, and the number of waves is called run length. The statistical analysis of runs in the wave record permits to derive information about the persistence of wave groupiness [31].

The second approach to analyze wave groupiness considers the sequence of ocean waves as a Markov chain. In this ap-

proach, the correlation coefficient γ between two waves is a key parameter. As γ is directly related to the expected number of waves per run, it is a good statistical measure to characterize wave groupiness. The respective theory was first introduced in [32] and subsequently improved in [33] and [8], where γ was expressed as a function of the frequency spectrum $S(f)$. There are additional 1-D grouping parameters used in the literature that can be derived from the spectrum, like the peakedness parameter Q_p [29]. The role of the peakedness of the spectrum in generating extreme waves is discussed in [34]. The exact definition of Q_p and γ is given in the Appendix. It has to be mentioned that the numerical calculation of Q_p is instable due to its high dependency on the spectral sampling, especially when comparing different datasets [11].

V. Two-Dimensional Grouping Algorithm

In this section, the 1-D wave group analysis presented in Section III is extended to the 2-D case. A new wavelet-based algorithm is presented to estimate ocean wave group parameters from SAR images.

The wavelet transform of a SAR image $I(\mathbf{x})$ is defined as

$$\mathcal{W}_\psi I : (a, \mathbf{b}) \mapsto \frac{1}{|a|} \int_{\mathbb{R}^2} I(\mathbf{x}) \psi \left(\frac{\mathbf{x} - \mathbf{b}}{a} \right) d^2\mathbf{x} \qquad (3)$$

where a is the scaling parameter ($\neq 0$) and $\mathbf{b}$ is a 2-D vector. The wavelet function ψ has to satisfy certain smoothness and normalization criteria which are described in [35]. Unlike the classical Fourier analysis, the wavelet transform provides spatial information on the frequency distribution and is, therefore, known as an efficient tool in image analysis [36].

The wave group analysis described here is based on an edge detection method presented in [18] and [37]. As an illustration the wavelet transform of the simulated wave groups in Fig. 3 is shown at the bottom of the same Figure. The wavelet scales $a \in [1, 64]$ correspond to the inverse frequency and are plotted in logarithmic scale. For the spline wavelet used here and an image resolution of 20 m, the maximum response of a homogenous wave of length λ is at scale $a \approx \lambda/50$ m. It can be clearly seen that a change of the local wavelength within the groups is reflected by a shift of energy along the scale axis; with the waves getting longer, the energy of the wavelet transform is shifted to longer spatial scales.

It can be seen as well that the wavelet transform is 90° phase shifted with respect to the image wave patterns. As these patterns are in turn 90° phase shifted with respect to the sea surface elevation (compare Section III), the local extrema of the wavelet transform match the troughs and crests of the ocean waves. More precisely the local wavelet maxima indicate local curvature extrema in the ocean wave field. As for narrow banded spectra the local curvature maxima are highly correlated with local elevation maxima, a thresholding of the wavelet transform is to some extent equivalent to a thresholding of the wave envelope as, e.g., proposed in [31]. It has to be emphasized that this is only true for range traveling waves. According to the wavelet theory, these extreme values of the wavelet transform correspond to irregular features in the signal, e.g., image edges [35].

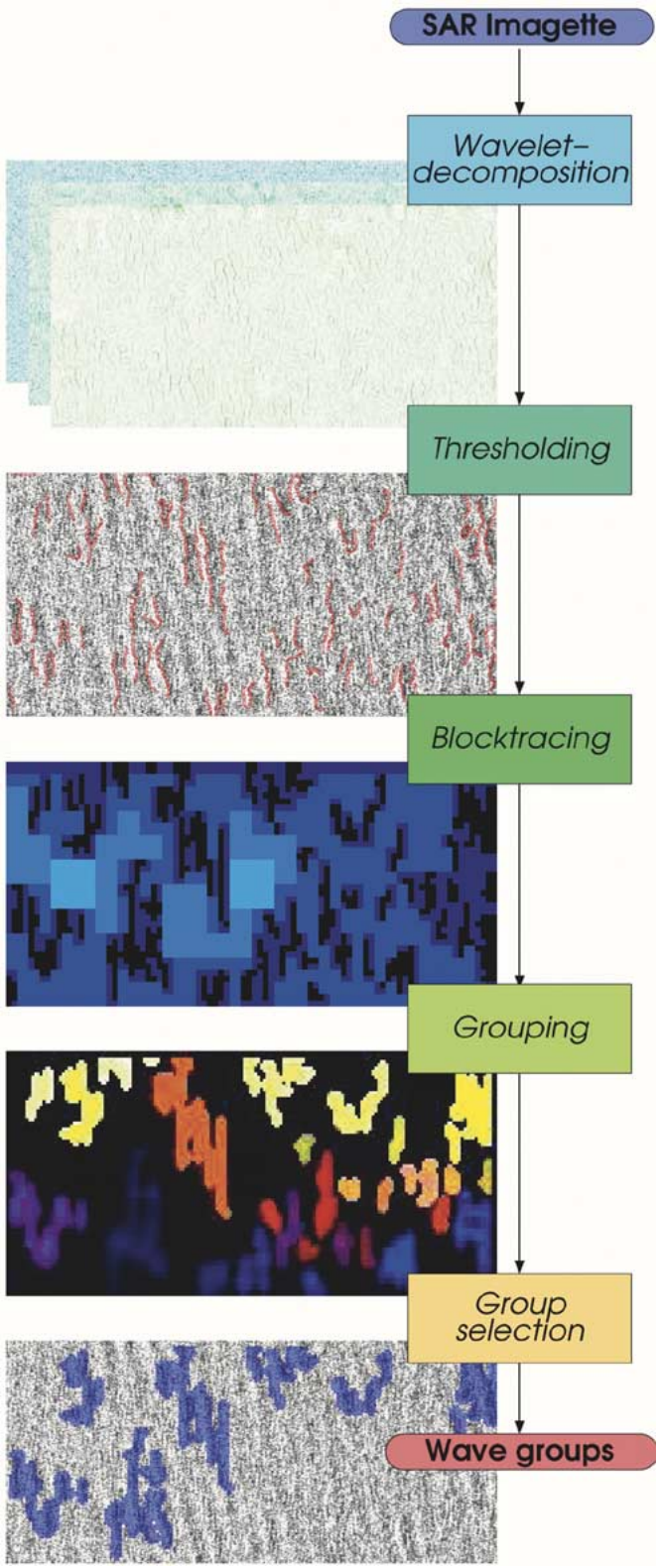

Fig. 4. Flowchart of the wavelet-based group analysis method.

A flowchart of the algorithm given here is presented in Fig. 4. The first step of the proposed wavelet algorithm is the detection of high waves corresponding to steep edges in the SAR image. Wavelet edge detection has been shown to be theoretically equivalent to the SAR specific Touzi edge detector [38] under certain circumstances (using the pointwise logarithm of

SAR images with the Haar wavelet ψ_H with adapted support and assuming homogenous speckle [39]). For reasons of computational efficiency, the wavelet transform (3) is calculated on dyadic wavelet scales ($a = 2^k, k = 0, 1, \ldots$) without subsampling using Mallat's redundant discrete wavelet transform algorithm [37], i.e., a specific iterative filter convolution (in our case the spline wavelet filter was used). It is applied to the five-look amplitude density image (pointwise logarithm of the amplitude image) with square 20×20 m^2 pixels.

The edge detection method is based on the analysis of the wavelet transform modulus maxima (WTMM), which are defined as the local maxima of $|\mathcal{W}_\psi I|$ along lines of constant scale a. It was shown in [35] that the decay properties of $|\mathcal{W}_\psi I(a, b)|$ along the respective lines $(a, \mathbf{b}(a))$ correspond to different types of image singularities. The algorithm proposed here is based on this relationship, the discretization exactly follows [37].

The WTMM of the first three scales ($a = 2^0, 2^1, 2^2$) are displayed as an image stack in the top part of Fig. 4. The method is applied to an ERS-2 SAR imagette acquired on September 7, 1996 at 9:51:16 UTC with image center at $46°50'$ S, $3°31'$ W. The image shows an almost range traveling swell system with wavelength $\lambda = 451$ m and propagation direction $\varphi = -171°$ (anticlockwise versus range).

A thresholding of the WTMM is used to separate edges associated with high and steep waves from SAR image speckle noise. It was shown in [39] that this procedure is a robust and efficient method to detect edges in the underlying (noise free) radar cross section (RCS) pattern. An additional property of the method is that it only keeps the strongest edges, i.e., between regions of a high RCS ratio (the ones showing high contrast) corresponding to the highest waves (see second image in Fig. 4). The threshold value T_ψ is chosen adaptively from the strength distribution in order to keep only the strongest edges in the image according to

$$T_\psi = \mu_\psi + 2.5 \cdot \sigma_\psi \tag{4}$$

where μ_ψ is the mean value of the WTMM image on scale $a = 2^2$, and σ_ψ is the respective standard deviation.

Taking results from the 33 000 imagette dataset the maximal WTMM values show good correlation (0.7 to 0.8) to the maximum wave steepness and crest to trough waveheight on a SAR imagette when using the quasi-linear SAR inversion algorithm presented in [40]. The significant waveheight from this inversion is correlated to the threshold T_ψ at a correlation of 0.92.

A direct thresholding in the image is not possible due to two reasons. First, the high speckle noise level causes the need of an adaptive smoothing process usually more complicated than the wavelet filtering. On the other hand, the image intensity is very much dependent on the wind speed. Using wavelet techniques, the information from exactly the right scale between large-scale wind variations and small-scale speckle noise can be extracted.

In the next step of the wave grouping algorithm, the strong edges are combined to groups by a so-called blocktracing algorithm (BA). BA [18] is a region growing algorithm to separate regions of high and low edge density: starting with large, edge-free square regions, small neighboring squares are attached recursively. This allows to identify edge-free regions and yields

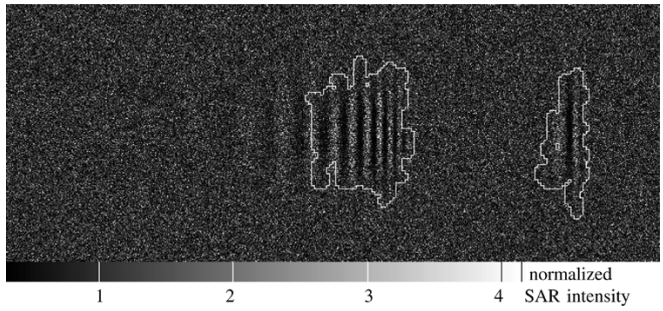

Fig. 5. Wave groups as detected by applying the wavelet technique to a simulated SAR image (see text for details).

contiguous areas with edges resulting from groups of big waves. In order to avoid artefacts, the initial size of the blocks is chosen large enough to contain at least one complete wave. For a typical wavelength of about 250 m in the open ocean, a start block size of 48×48 pixel (about 1 km^2) turned out to be a robust choice. Edge-free regions of shrinking size are added iteratively in a neighborhood down to a size of 6×6 pixel still large enough to keep the single waves of the group runs connected. After each pass of the algorithm the remaining unmarked squares are split into four smaller ones of half width and height and a new region filling is started at the borders between marked and unmarked squares. In the corresponding image of Fig. 4, the different shades of blue mark the different iteration steps and block sizes.

After the region growing algorithm has terminated resulting in a separation of the entire wave field in areas of high and low edge density a final smoothing operation is carried out. Boxes of the next smaller size (3×3 pixel) are added to the high edge density regions leading to smoother boundaries of the group areas, which are at the same time slightly enlarged.

Finally, a thresholding for the group area is used to remove spurious groups. A group run area threshold $T_A = 8.0 \cdot 10^5$ m^2 was used here, which corresponds to 10^4 pixels of an ERS-2 single-look complex (SLC) SAR image. For the mean wavelength of about 250 m (average over some 33 000 imagettes), this means a group area of about three wavelengths at 1 km width.

Again, using the SAR inversion and a wave grouping algorithm based on the historic group definition for comparison gave a good agreement in group size, shape and location.

The resulting groups for the example shown in Fig. 4 can be seen at the bottom of the same figure. The seven groups found have a total area of 9.2 km^2 (18.4% of the whole imagette). Small areas with strong edges (i.e., from a single high wave like the one close to the middle of the imagette in Fig. 4) are removed by the group area thresholding procedure.

As a second example we use the sea surface using the range traveling wave groups from Fig. 3 extended to 2-D with a Gaussian decay in the cross propagation direction. In addition, speckle noise was simulated assuming a typical five-look averaged SAR image. Fig. 5 gives the results using the algorithm described above.

When doing the same without speckle the group shape is constant azimuthal direction. The intervals of the groups within the 1-D signal are indicated by two gray bars in Fig. 3. Looking

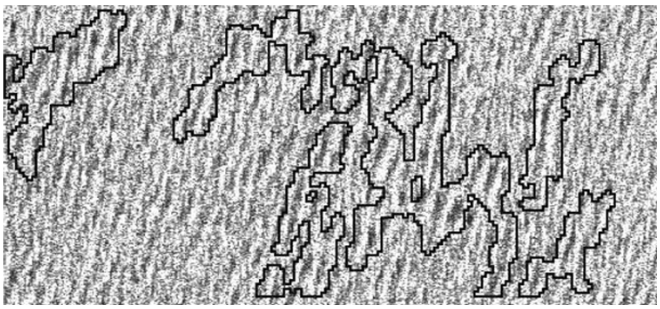

Fig. 6. Groups found in the imagette from Fig. 1(c).

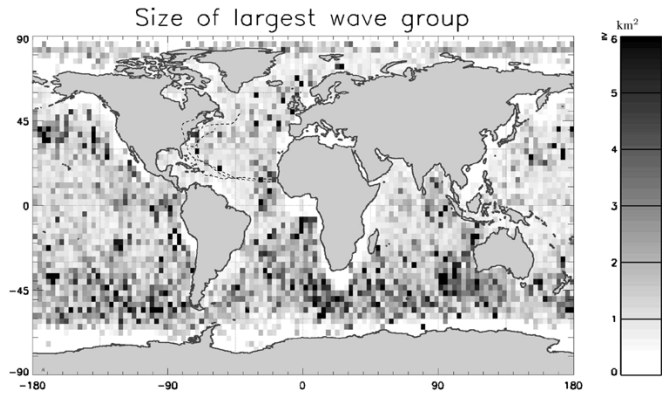

Fig. 7. Map with maximum group size. Especially the rough areas in the southern hemisphere and the path of the three hurricanes (dashed lines) during the recording period in the Northern Atlantic are visible. The time period is the whole imagette dataset from Table I.

at the original sea surface one has to mention the symmetry of the detected group as a quality feature of the proposed algorithm. The threshold wave height for the groups in this example is $H_T \approx 1.4$ m, which is between mean and significant waveheights ($H_T \approx 1.3\overline{H} \approx 0.7H_s$) which is comparable to classical 1-D group run definitions [31].

The algorithm presented above only takes into account information from the SAR image itself. It is both independent of assumptions on the SAR imaging process and from additional information, e.g., from wave models or measurements for calibration. These would be needed for an algorithm based on a SAR inversion scheme like described in [40].

The area of the group runs detected with the wavelet algorithm is connected but not necessarily simply connected (i.e., they can contain holes) and by far not convex as one might expect looking at 1-D wave groups (compare Fig. 6). However, the frequency of groups with holes is negligible compared to the occurrence of simply connected groups. The 2-D group shape usually is also not aligned with the dominant wave or crest direction. Furthermore, 1-D cuts through a 2-D wave group can produce two or more different runs in terms of the 1-D definition. In general, the group structure in two dimensions is much more complicated than one could imagine from the 1-D point of view and it seems that more theoretical investigations are required to better understand the 2-D aspects of realistic wave fields. The upcoming availability of new radar data suitable for statistical analysis of 2-D wave fields will certainly be a driver for investigations on this topic. The proposed algorithm is seen as an efficient analysis tool in this context.

VI. Application to Global Data

The radar dataset introduced in Section II enables the analysis of 2-D wave fields on a global scale for the first time. In this section, the proposed wavelet algorithm is applied to these radar data to investigate the global distribution as well as the statistics of different group parameters. It is well known that wave grouping is an important factor in the generation of extreme waves [41], [42]. Maps of regions with high group activity can, therefore, help to identify regions of high risk for ship navigation and offshore operations. Different studies on the detection of freak waves using new remote sensing techniques have been carried out based on both spaceborne [43], [44] and ground-based radar sensors [45].

Prior to applying the wavelet algorithm to the entire dataset, images with inhomogeneous features caused by land, sea ice or atmospheric features were sorted out using the algorithm described in [40]. Also the nonlinearity degree of the waves (1), [22] has to be taken into account. Group parameters were then calculated for the remaining 22 500 imagettes. Global maps giving information on the number of groups in each image as well as the respective maximum group size were generated. For larger group sizes, there usually are more extreme waves within the group run which increases the risk for ships. Fig. 7 presents a map of the maximum group size found in the imagettes acquired within a $3^\circ \times 3^\circ$ box. The map shows higher group activities due to heavy seas in the Southern Hemisphere (as most of the imagettes were taken in southern winter with strong winds in the southern oceans) as well as along the path of the hurricanes in the North Atlantic during the 1996 hurricane season. The extreme cases in the northern Pacific ocean (between Hawaii and Alaska) occur in a region passed by several typhoons in the three-week period. Most extreme situations on the southern hemisphere appear in stormy areas of 40° to 60° latitude, a few others can be explained as swell leaving this band. Thus at least from a statistical point of view the parameter "group size" is a measure for danger by wave groups, e.g., coming from storm systems.

Additional parameters like the maximum or mean wave crest length are of interest for various applications. Effects of severe weather conditions like hurricanes in the North Atlantic are clearly visible in these parameters, too. Creating a series of maps like the one in Fig. 7 with different time spans, one can even see the path of the hurricane represented by areas with long crested waves and high grouping propagating across the northern part of the Atlantic Ocean from Cape Verde to the east coast of the U.S. and back to the Azores (see http://www.dlr.de/caf/institut/imf/organisation/imf_oe_gw/x_images/crestmovie.gif for WWW example).

For statistical comparisons, several parameters from collocated ECMWF WAM spectra were calculated, including the peakedness parameter Q_p and the wave height correlation coefficient γ (compare Appendix A). Maps of these parameters are given in Fig. 8. They show the same structures from storm systems (Hurricanes, northern Pacific, Southern Hemisphere) [46].

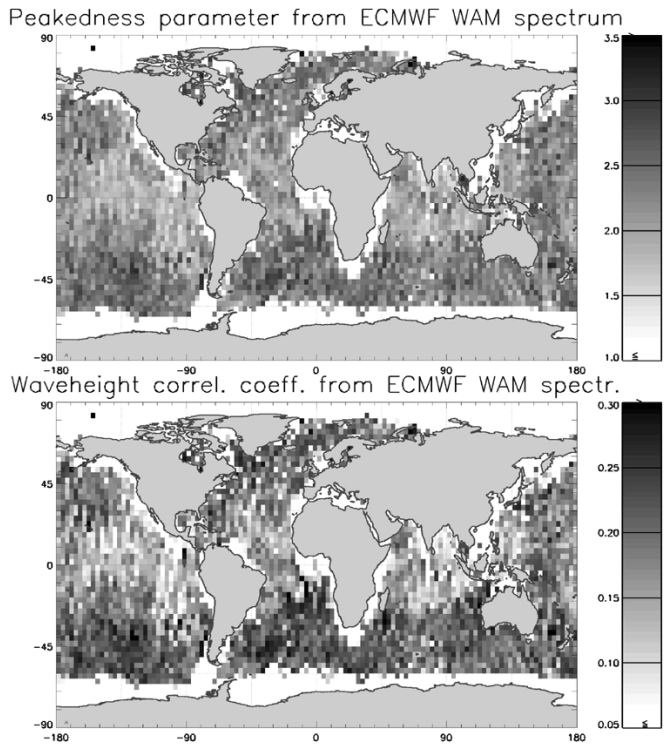

Fig. 8. Global maps of the classical group parameters Q_p and γ calculated from collocated ECMWF WAM spectra for the time period given in Table I.

Thus, at least from a statistical point of few the newly defined group parameters using the algorithm presented are a valid generalization of some historic wave group definition using Q_p or γ.

VII. Analysis of Wave Groups in Coastal Areas

Apart from the global analysis presented in the last section the proposed algorithm is also an efficient tool for a detailed investigation of the spatial dynamics of wave groups in coastal areas. These regional studies can be ideally performed using ERS-2 image mode scenes of 100 × 100 km size with a resolution of about 20 × 20 m.

An example of group detection on large ocean areas can be seen in Fig. 9. This figure shows the northern part of the German island of Sylt in the North Sea. The image was taken by the ERS-2 satellite on October 15, 1998 at 10:25 UTC and shows an area of about 32×22 km^2. WNW winds at $u \approx 13$ m/s were measured at Sylt 1.5 h later. The image shows waves of about 100 m wavelength from the same direction with strong spatial dynamics of the wave field mainly due to the variable bathymetry. As suggested by the standard ocean wave theory [47], [48], the wavelength is getting shorter as the waves enter the shallow water region close to the coast.

Due to the changing water depth the wave grouping is changing as well. As the waves enter shallower water, according to linear wave theory [31], the relative spectral bandwidth is increasing, which is equivalent to a decrease of the spectral peakedness. In the spatial domain, this means that the correlation between consecutive waves decreases and thus the average number of waves per group is getting smaller.

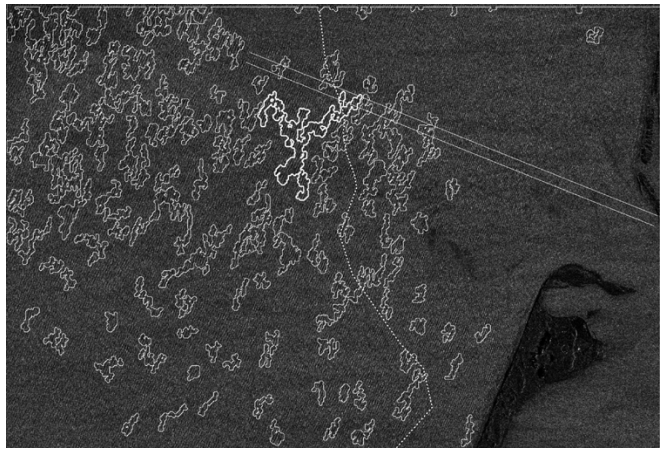

Fig. 9. Wave groups detected by the wavelet technique on an ERS-2 image mode SAR image near the island Sylt (Oct. 15, 1998, 10^{26} UTC, image center: $55.1°$ N, $8.2°$ E, 32×22 km^2). WNW winds at 13 m/s were measured. The two lines mark the border of the region averaged for the cut in Fig. 10. The dotted line is the line of 10 m waterdepth coarsely digitized from a nautical chart.

Applying the wave group detection algorithm proposed in this work, it can be seen in Fig. 9 that the number of groups per area is clearly decreasing as the waves approach the coast. In fact, the boundary of the area with high group activity at the top right of the image is in good agreement with the 10 m waterdepth isoline (dotted line in Fig. 9). It is also obvious that the largest groups appear in deeper water. It is interesting to note that the largest group found on the image (≈ 15 km^2) indicated by a thick boundary is in the region where the number of waves per area starts to decrease.

As wave grouping is the key factor in wave energy propagation, this analysis of wave groups approaching coastal areas permit to evaluate the impact of wave fields on the coastal morphodynamics being also able to form extreme (mad-dog) waves [42]. For the island of Sylt, these processes are of high commercial relevance. It is expected that a detailed analysis of wave group parameters from a larger dataset covering various sea state conditions can help to optimize coastal protection, i.e., the design and positioning of wave breakers.

The linearized approach is possible as the measured wind speed u and the waveheight of a fully developed wind sea yields $H_s < 3.6$ m and thus $C_{\text{lin}} < 0.2 \ll 0.7$ (cf. (1)).

In addition, a 1-D cut through the waves approaching the coast has been examined. To reduce speckle a 40 pixel wide band in the SAR image was averaged as depicted in Fig. 9. The two plots in Fig. 10 refer to the first and second half of the cut. Clear tendencies are visible in the graphs: The grouping activity is higher in the offshore area (top/left) and the waves are longer there. In addition, the 1-D wavelet transform is given. The wavelet transform shows the same tendencies: The center of gravity along the wavelet scales (considering only reasonable wavelengths/scales, e.g., $a < 8$) is slightly shifting upwards to lower scales/shorter waves toward the coast.

VIII. Conclusion and Outlook

A new efficient wavelet-based method was presented to estimate ocean wave group parameters from 2-D radar images.

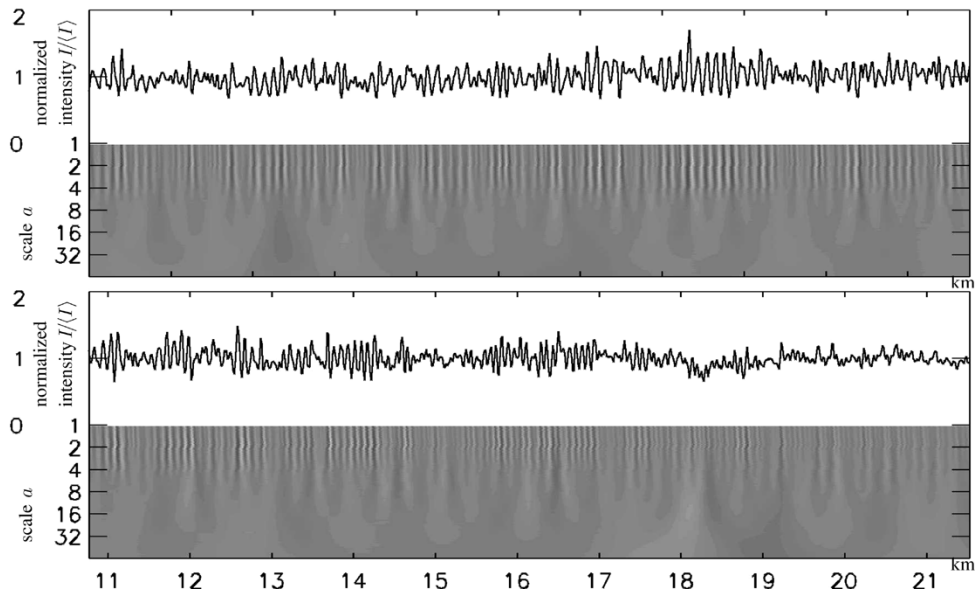

Fig. 10. Cut through the SAR image in Fig. 9 with corresponding wavelet transform. The ocean wavelength λ is related to the wavelet scale a by $\lambda \approx a \cdot 50$ m).

A brief outline of the classical 1-D wave grouping theory was given, and the development of 2-D analysis techniques was motivated.

The method was introduced using synthetic ocean surfaces and simulated SAR data including speckle noise. It was shown that the technique is able to recover the basic group structure, i.e., the group size and the relative position of the groups at least in those cases where the waves are propagating in near range direction.

The technique was applied to spaceborne SAR data on both global and regional scale. A new dataset of reprocessed ERS-2 wave mode images was used, which is so far the only source of 2-D spatial ocean wave information on a global basis. Maps of characteristic group parameters, such as the area of the largest group within images of fixed size, were presented. It was shown that the global distribution of the wavelet-derived parameters is in good agreement with classical 1-D parameters derived from colocated numerical wave model spectra. Respective global maps of the wave height correlation parameter γ and the peakedness parameter Q_p were presented. However, some deviations were found that are at least partly due to the fact that the grouping structure is not fully represented by the wave spectrum used as basis for the classical parameters.

The application of the wavelet technique to an ERS-2 image mode scenes demonstrated the potential of the method to analyze the spatial dynamics of ocean wave grouping in coastal areas with strong water depths variations. Furthermore, the wavelet transform proved to be a robust tool to analyze wavelength changes of waves entering shallow water areas. The importance of these observations for coastal protection was discussed.

The study is one of the first attempts to analyze both the global and the regional dynamics of 2-D group properties. There is need for further analysis to fully understand the implications concerning wave physics and radar imaging limitations. It is planned to apply the method to 2-D marine radar images, which are less affected by motion effects and which allow a closer insight into the time-space structure of wave grouping. Another plan is to extend the global analysis of wave group parameters to a larger dataset covering more seasons and extreme events like hurricanes. This will lead to more robust statistical results and help to better understand the physical nature of wave grouping and its dependence on the oceanic and atmospheric boundary conditions such as currents or cyclones.

After reprocessing is finished, there will be more than ten years of wave mode data available from the ERS-1 and ERS-2 satellites that can be used for ocean wave analysis on a decadal basis. Wave mode data acquisitions are continued by the new ENVISAT satellite, which is acquiring images every 100 km along the track. The presented wavelet technique is applicable to ENVISAT data without change.

It is expected that the importance of analysis and measurement techniques for 2-D group parameters will grow significantly in the future. This is because the procedures used in up-to-date design of marine structures like ships or offshore platforms require detailed information on the 2-D sea surface to assess the respective structure responses. Furthermore, there are strong indications that grouping properties play a role in the generation of extreme waves, which are one of the key factors in the design of safe marine structures.

APPENDIX
DEFINITIONS OF SOME HISTORIC SPECTRAL WAVE PARAMETERS

As shown in [8], the correlation γ of two subsequent waves can be expressed as

$$\gamma = \frac{E(\kappa) - \frac{(1-\kappa^2)K(\kappa)}{2} - \frac{\pi}{4}}{1 - \frac{\pi}{4}} \tag{5}$$

where $E(\kappa)$ and $K(\kappa)$ are complete elliptic integrals of first and second kind, respectively. The parameter κ in (5) depends on the mean separation time τ between two waves. This parameter

can be estimated for a characteristic time $\tau = T_e = m_0/m_1$ (where m_0 and m_1 are the zeroth and first spectral moments, respectively) using the expression [8]

$$\kappa = \left| \frac{1}{m_0} \int_0^\infty S(f) e^{i2\pi f T_e} df \right|. \tag{6}$$

Equations (5) and (6) enable the computation of γ from the wave spectrum.

Analyzing wave records, it can be seen that the number of waves per group increases with decreasing width of the frequency spectrum $S(f)$. The peakedness of the spectrum is thus strongly linked with the grouping of waves. In [29], the parameter Q_p defined as

$$Q_p = \frac{2}{m_0^2} \int_0^\infty f S^2(f) df \tag{7}$$

was proposed as a suitable quantity to characterize the peakedness. The parameter varies from 1 to around 2 for wind waves and values greater than 2 for swell [11], [31]. The numerical estimation of Q_p is very sensitive to the frequency resolution of $S(f)$. Though this problem occurs as well for the estimation of the parameter κ given by (6), the numerical computation of κ (and therefore γ) is less sensitive than Q_p [31].

ACKNOWLEDGMENT

The authors would like to thank B. Schättler for processing the wave mode data and H. Dankert for helpful discussions. The wave model data was provided by the ECMWF. The authors would like to thank the European Space Agency for providing ERS-2 SAR wave mode raw data in the framework of the ERS A03 project COMPLEX (ID 192).

REFERENCES

[1] C. C. Piotrowski and J. P. Dugan, "Accuracy of bathymetry and current retrievals from airborne optical time-series imaging of shoaling waves," *IEEE Trans. Geosci. Remote Sens.*, vol. 40, no. 12, pp. 2606–2618, Dec. 2002.

[2] J. C. Nieto Borge, G. R. Rodríguez, K. Hessner, and P. I. González, "Inversion of nautical radar images for surface wave analysis," *J. Atmos. Oceanic Technol.*, vol. 21, no. 8, pp. 1291–1300, 2004.

[3] C. C. Piotrowski and J. P. Dugan, "Accuracy of bathymetry and current retrievals from airborne optical time-series imaging of shoaling waves," *IEEE Trans. Geosci. Remote Sens.*, vol. 40, no. 12, pp. 2606–2618, Dec. 2002.

[4] J. C. Nieto Borge, S. Lehner, A. Niedermeier, and J. Schulz-Stellenfleth, "Detection of ocean wave groupiness from spaceborne synthetic aperture radar," *J. Geophys. Res.*, vol. 109, 2004.

[5] W. Rosentahl, S. Lehner, H. Dankert, H. Günther, K. Hessner, J. Horstmann, A. Niedermeier, J. C. N. Borge, J. Schulz-Stellenfleth, and K. Reichert, "Detection of extreme single waves and wave statistics," in *Proc. MAXWAVE Final Meeting*, Geneva, Switzerland, Oct. 8–10, 2003.

[6] H. E. Krogstad, J. Liu, H. Socquet-Juglard, K. B. Dysthe, and K. Trulsen, "Spatial extreme value analysis of nonlinear simulations of random surface waves," in *Proc. 23rd Int. Conf. Offshore Mechanics and Arctic Engineering*, Vancouver, BC, Canada, Jun. 2004.

[7] V. I. Piterbarg, "Asymptotic methods in the theory of gaussian processes and fields," *AMS Transl. of Math. Monographs*, vol. 148, 1996.

[8] M. S. Longuet-Higgins, "Statistical properties of wave groups in a random sea-state," *Philos. Trans. R. Soc. Lond.*, vol. 312, pp. 219–250, 1984.

[9] M. S. Longuett-Higgins, *Wave Group Statistics*. Dordrecht, The Netherlands: Reidel, 1986, pp. 15–35.

[10] J. Hamilton, W. H. Hui, and M. A. Donelan, "A statistical model for groupiness in wind waves," *J. Geophys. Res.*, vol. 84, pp. 4875–4884, 1979.

[11] M. K. Ochi, *Ocean Waves. The Stochastic Approach*. Cambridge, U.K.: Cambidge Univ. Press, 1998.

[12] A. Marón, "Wave groups on wave records measured along spanish shores," in *Proc. 21st Int. Conf. Coastal Engineering*, Torremolinos, Spain, 1988.

[13] R. T. H. J. R. Medina, "A review of the analyses of ocean wave groups," *Coastal Eng.*, vol. 14, pp. 515–542, 1990.

[14] E. Mollo-Christensen and A. Ramamonjiarisoa, "Modeling the presence of wave groups in random wave field," *J. Geophys. Res.*, vol. 83, no. C8, pp. 4117–4122, 1978.

[15] W. Alpers and K. Hasselmann, "The two-frequency microwave technique for measuring ocean wave spectra from an airplane or satellite," *Boundary-Layer Metereol.*, vol. 13, pp. 215–230, 1978.

[16] K. Hasselmann and S. Hasselmann, "On the nonlinear mapping of an ocean wave spectrum into a synthetic aperture radar image spectrum," *J. Geophys. Res.*, vol. 96, pp. 10 713–10729, 1991.

[17] P. Heimbach, S. Hasselmann, and K. Hasselmann, "Statistical analysis and intercomparison with WAM model data of three years of global ERS-1 SAR wave mode spectral retrievals," *J. Geophys. Res.*, vol. 103, pp. 7931–7977, 1998.

[18] A. Niedermeier, E. Romaneessen, and S. Lehner, "Detection of coastlines in SAR images using wavelet methods," *IEEE Trans. Geosci. Remote Sens.*, vol. 38, no. 5, pp. 2270–2281, Sep. 2000.

[19] S. Lehner, B. Schättler, J. Schulz-Stellenfleth, and H. Breit, "Processing and calibration of ERS SAR single look complex imagettes—Extraction of wind and sea state parameters," in *Proc. CEOS SAR Calibration and Validation Workshop*, Noordwijk, The Netherlands, 1998.

[20] W. R. Alpers and C. L. Rufenach, "The effect of orbital motions on synthetic aperture radar imagery of ocean waves," *IEEE Trans. Antennas Propag.*, vol. AP-27, no. 4, pp. 685–690, Jul. 1979.

[21] K. Hasselmann, R. K. Raney, W. J. Plant, W. Alpers, R. A. Shuchman, D. R. Lyzenga, C. L. Rufenach, and M. J. Tucker, "Theory of synthetic aperture radar ocean imaging: A MARSEN view," *J. Geophys. Res.*, vol. 90, pp. 4659–4686, 1985.

[22] C. Brüning, W. Alpers, and K. Hasselmann, "Monte-Carlo simulation studies of the nonlinear imaging of a two dimensional surface wave field by a synthetic aperture radar," *Int. J. Remote Sens.*, vol. 11, pp. 1695–1727, 1990.

[23] G. Neumann and W. J. Pierson, Jr, *Principles of Physical Oceanography*. Englewood, NJ: Prentice-Hall, 1966.

[24] J. A. Ewing, "Mean length of runs of high waves," *J. Geophys. Res.*, vol. 78, no. 12, pp. 1933–1936, 1973.

[25] S. K. Chakrabarti, R. H. Snider, and P. H. Feldhausen, "Mean length of runs of ocean waves," *J. Geophys. Res.*, vol. 79, no. 36, pp. 5665–5667, 1974.

[26] K. G. Nolte and F. H. Hsu, "Statistics of ocean wave groups," in *Proc. 4th Offshore Technol. Conf.*, vol. 2, 1972, pp. 637–644.

[27] M. K. Rye, "Wave group formation among strom waves," in *Proc. Conf. Coastal Engineering*, vol. 1, 1974, pp. 164–83.

[28] ——, "Wave parameter studies and wave groups," in *Proc. Conf. Sea Climatology*, 1979, pp. 89–123.

[29] Y. Goda, "Numerical experiment on wave statistics with spectral simulation," *Rep. Port Harbour Res. Inst. 9*, vol. 3, pp. 3–57, 1970.

[30] ——, "On wave groups," in *Proc. Conf. Behavior Offshore Structures*, vol. 1, 1976, pp. 1–14.

[31] ——, *Random Seas and Design of Maritime Structures*. Tokyo, Japan: Univ. Tokyo Press, 1995.

[32] A. Kimura, "Statistical properties of random wave groups," in *Proc. 17th Int. Conf. Coastal Engineering*, vol. 3, Sydney, Australia, 1980, pp. 2955–2973.

[33] J. A. Battjes and G. P. van Vledder, "Verification of kimura's theory for wave group statistics," in *Proc. 19th Coastal Engineering Conf.*, vol. 1, Houston, TX, 1984, pp. 642–648.

[34] P. A. E. M. Janssen, "Nonlinear four wave interactions and freak waves," *J. Phys. Oceanography*, vol. 33, no. 4, pp. 863–884, Apr. 2003.

[35] S. G. Mallat and W. L. Hwang, "Singularity detection and processing with wavelets," *IEEE Trans. Inform. Theory*, vol. 38, no. 2, pp. 617–643, Mar. 1992.

[36] I. Daubechies, *Ten Lectures on Wavelets*. Philadelphia, PA: SIAM, 1992.

[37] S. G. Mallat and S. Zhong, "Characterization of signals from multiscale edges," *IEEE Trans. Pattern Anal. Mach. Intell.*, vol. 14, no. 7, pp. 710–732, Jul. 1992.

[38] R. Touzi, A. Lopes, and P. Bousquet, "A statistical and geometrical edge detector for SAR images," *IEEE Trans. Geosci. Remote Sens.*, vol. 26, no. 6, pp. 764–773, Nov. 1988.
[39] A. Niedermeier, "Wavelet-Methoden in der SAR-Bildverarbeitung—Ein Wavelet-basiertes Wasserstandslinienverfahren zur Topographiebestimmung im Wattenmeer," Ph.D. dissertation, Tech. Univ. München, Munich, Germany, 2002.
[40] J. Schulz-Stellenfleth and S. Lehner, "Measurement of two-dimensional sea surface elevation fields from complex synthetic aperture radar data," *IEEE Trans. Geosci. Remote Sens.*, vol. 42, no. 6, pp. 1144–1160, Jun. 2004.
[41] A. K. Magnusson, M. A. Donelan, and W. M. Drennan, "On estimating extremes in an evolving wave field," *Coastal Eng.*, vol. 36, pp. 147–163, 1999.
[42] M.-Y. Su, Y.-C. Lin, C.-H. Tsai, and H.-M. Tseng, "Nonlinear dynamical mechanisms connecting ocean giant waves and wave groups," in *Proc. Offshore Mechanics and Arctic Engineering Conf.*, 2002, pp. 6–6.
[43] S. Lehner, J. Schulz-Stellenfleth, A. Niedermeier, J. Horstmann, and W. Rosenthal, "Detection of extreme waves using synthetic aperture radar images," in *Proc. IGARSS*, Toronto, ON, Canada, Jun. 2002.
[44] J. Schulz-Stellenfleth, S. Lehner, and D. Hoja, "Use of the coherence of synthetic aperture radar cross spectra for ocean wave measurements," in *Proc. IGARSS*, Toronto, ON, Canada, Jun. 2002.
[45] H. Dankert, J. Horstmann, and W. Rosenthal, "Detection of extreme ocean waves using radar-image sequences," in *Proc. IGARSS*, Toronto, ON, Canada, 2002.
[46] J. Horstmann, P. Vachon, S. Lehner, and D. Hoja, "SAR measurements of ocean wind and wave fields in hurricanes," in *Proc. IGARSS*, vol. 1, Toulouse, France, Jul. 2003, pp. 230–232.
[47] O. Phillips, *Dynamics of the Upper Ocean*. Cambridge, U.K.: Cambridge Univ. Press, 1977.
[48] R. M. Sorensen, *Basic Wave Mechanics for Coastal and Ocean Engineers*. New York: Wiley, 1994.

Andreas Niedermeier studied mathematics at the Munich University of Technology (TUM), Munich, Germany, from 1993 to 1998. His diploma thesis dealt with implementation of sparse grid prewavelet methods for PDEs. He graduated in the program "Angewandte Algorithmische Mathematik," TUM from 1998–2001. He received the Ph.D. degree from TUM in 2002. His thesis was on wavelet methods in SAR image processing.

He is currently working as a Postdoctoral Researcher at the German Aerospace Center, Oberpfaffenhofen.

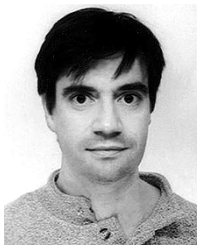

José Carlos Nieto Borge received the B.A. degree from the Universidad Complutense de Madrid (UCM), Madrid, Spain, in 1988, and the Ph.D. degree from the Universidad de Alcalá de Henares, Madrid, both in physics. His Ph.D. thesis was on the analysis of ocean waves by using temporal sequences of marine radar sea surface images.

In 1989, he started to work in ocean wave analysis in the Department of Climate and Maritime Research of the Spanish Harbor Administration. From 1997 to 1998, he was a Guest Scientist with the GKSS-Research Center. In 2002, he joined the German Aerospace Center, Oberpfaffenhofen.

Susanne Lehner (M'01) received the M.S. degree in applied mathematics from Brunel University, Uxbridge, U.K., in 1979, and the Ph.D. degree in geophysics from the University of Hamburg, Hamburg, Germany, in 1984.

She was a Research Scientist with the Max-Planck Institute for Climatology, Hamburg, and in 1996, she joined the German Aerospace Center (DLR), Oberpfaffenhofen. She was a Research Scientist in the marine remote sensing at the DLR Remote Sensing Technology Institute, working on the development of algorithms determining marine parameters from SAR. She is currently a Professor at the Rosenstiel School of Marine and Atmospheric Science, University of Miami, FL. Her main scientific interest is the derivation of maritime parameters from ERS SAR images.

Johannes Schulz-Stellenfleth received the Diploma degree in applied mathematics and the Ph.D. degree from the University of Hamburg, Hamburg, Germany, in 1996 and 2003, respectively.

He joined the German Aerospace Center (DLR), Oberpfaffenhofen, Germany, in late 1996. He was a Research Scientist with the Remote Sensing Technology Institute (IMF), DLR and is currently Head of the radar oceanography group. The main interest of his present work is the use of complex SAR data to derive two-dimensional ocean wave spectra. Apart from that, he is working on the application of cross-track interferometric data to measure sea surface elevation models.